Recent Science and Technology 18(1): 266457

Recent Science and Technology

Journal homepage: https:// www.tci-thaijo.org/index.php/rmutsvrj/index

ISSN: 3057-0786 (Online)

Research Article

Application of Silver/Carbon-based Composite Nanofiber Membrane for Improvement of Microfiltration System

Tanayt Sinprachim [a*], Kattinat Sagulsawasdipan [b] and Somchai Sonsupap [c]

[a] *Department of General Education, Faculty of Science and Fisheries Technology, Rajamangala University of Technology Srivijaya, Sikoa, Trang 92150, Thailand.*

[b] *Department of Marine Science and Environment, Faculty of Science and Fisheries Technology, Rajamangala University of Technology Srivijaya, Sikoa, Trang 92150, Thailand.*

[c] *College of Innovation and Industrial Management, King Mongkut's Institute of Technology Ladkrabang, Ladkrabang, Bangkok 10520, Thailand.*

Article history:

Received: 2025-03-27
Revised: 2025-06-18
Accepted: 2025-08-04

Keywords:

Carbon composite;
Nanofibers;
Microfiltration;
Membrane;
Filtration

ABSTRACT

In this study, silver-reinforced carbon nanofiber membranes (CNF@Ag) were fabricated through a binder-free extrusion process. A precursor mixture of carbon nanofibers (CNF) and silver nitrate ($AgNO_3$) was extruded at 40 MPa, followed by sintering at 800°C in an argon atmosphere for 4 hours to enhance the membrane structure. The physical properties of the CNF@Ag membranes, including porosity, wettability, morphology, and microfiltration efficiency, were systematically analyzed. The results demonstrated that the CNF@Ag membranes exhibited effective microfiltration properties with pore sizes ranging from 9.21 to 21.99 nm. These membranes achieved a turbidity removal efficiency of up to 92.69%, indicating their potential as an effective pre-treatment step for seawater desalination. This study highlights the promising application of CNF@Ag membranes in water purification processes, particularly for turbidity removal in desalination systems.

1. Introduction

The rapid growth of the global population, coupled with the impacts of climate change, has significantly increased the demand for fresh and clean water, especially in urban areas (Flörke *et al.*, 2018). By 2025, many regions are expected to experience severe water shortages, threatening public health, economic stability, and social development (Boretti and Rosa, 2019). As a result, the efficient management of available water resources and the advancement of effective filtration technologies have become critical priorities in addressing global water crises (Brown *et al.*, 2015).

Microfiltration, a membrane filtration technology, has gained significant attention as a solution for improving water quality by removing particulate matter, bacteria, and other contaminants from water sources. Unlike desalination, which primarily targets the removal of salts from seawater or brackish water, microfiltration focuses on separating larger particles, microorganisms, and colloidal matter, making it a crucial process for ensuring access to safe drinking water in both urban and rural settings (Gude, 2016). Microfiltration is particularly advantageous due to its low energy consumption, cost-effectiveness, and scalability compared to other advanced water treatment methods such as reverse osmosis and distillation (Williams, 2022). However, challenges such as membrane fouling and contamination still hinder the efficiency and longevity of filtration systems, limiting their widespread use.

*** Corresponding author.**

E-mail address: *tanayt65@hotmail.com*

Cite this article as:

Sinprachima, T., Sagulsawasdipan, K. and Sonsupap, S. 2026. Application of Silver/Carbon-based Composite Nanofiber Membrane for Improvement of Microfiltration System**. Recent Science and Technology** 18(1): 266457.

https://doi.org/10.65411/rst.2026.266457

In response to these challenges, the incorporation of nanomaterials into membrane technologies has emerged as a promising approach to enhance filtration performance. Nanomaterials, particularly carbon-based nanocomposites, have shown great potential due to their high surface area, excellent porosity, and customizable properties (Gong *et al.*, 2024; Yang and Mi, 2013). These materials offer an enhanced filtration capacity and can be modified with nanoparticles such as silver (Ag) (Yu *et al.*, 2022; Andrade *et al.*, 2015) or titanium dioxide (TiO_2) (Davari *et al.*, 2021; Razmjou *et al.*, 2011; Rahimpour *et al.*, 2008) which impart antimicrobial properties, further improving the effectiveness of filtration systems against microorganisms.

Porous carbon-based nanocomposite materials, particularly those containing carbon nanofibers, have attracted considerable attention for their versatility and broad range of applications. These include uses in energy storage devices (e.g., supercapacitors, lithium-ion batteries, and hydrogen fuel cells) and biomedical fields (Levchenko *et al.*, 2023). In the context of water filtration, these materials have demonstrated great promise in reducing fouling and improving the overall filtration process, especially in applications requiring the removal of bacteria, suspended solids, and other contaminants (Noamani *et al.*, 2019; Idumah and Hassan, 2016; Oladunni *et al.*, 2018). Furthermore, carbon nanofibers, which are key components of these materials, can be fabricated using various methods, such as self-assembly, template synthesis (Pavlenko *et al.*, 2022), chemical vapor deposition (CVD) (Hulicova-Jurcakova *et al.*, 2008), and electrospinning (Inagaki *et al.*, 2012). Among these, electrospinning is particularly noteworthy for its ability to produce highly porous and uniform fibers with tunable properties, making it an ideal technique for fabricating advanced filtration membranes.

This study focuses on the development of carbon nanocomposite membranes containing varying ratios of silver nanoparticles (0, 10, 20, 40, and 200%) in carbon nanofiber composites (CNF, CNF@Ag-10, CNF@Ag-20, CNF@Ag-40, CNF@Ag200). This aims to address gaps in the use of CNF@Ag membranes for microfiltration, particularly in desalination and fouling resistance. While CNF-based membranes have shown potential in turbidity removal and microbial filtration, their effectiveness in removing salts from seawater and long-term stability remain underexplored. The impact of silver nanoparticle concentration on filtration performance was studied. Structural, chemical, surface, and porosity analyses of these membranes were conducted using techniques such as X-ray diffraction (XRD), Raman spectroscopy, scanning electron microscopy (SEM), transmission electron microscopy (TEM), and Brunauer-Emmett-Teller (BET) surface area analysis. The composite membranes were then evaluated in a comparative study to assess their ability to filter and improve the quality of contaminated water, focusing on key water quality parameters such as salinity, turbidity, odor, and color.

2. Materials and Methods

2.1 Preparation of metal oxide carbon nanocomposite fiber membrane material

Figure 1 illustrates the synthesis of carbon nanofibers reinforced with silver particles. Carbon nanofibers (CNF; Changsha Easchem. Co., Ltd, China) and silver nitrate ($AgNO_3$), Sigma-Aldrich, USA) were dissolved separately in ethanol at the ratios shown in Table 1 and stirred on a hot plate for at least 2 h to ensure that the carbon nanofibers were evenly distributed in ethanol and the silver nitrate was completely dissolved. Next, the two solutions were mixed together and stirred for another 2 h to obtain the CNF@$AgNO_3$ mixture, which was then dried at room temperature for 1 night and pressed into a membrane with a diameter of 26 mm using a hydraulic press at a pressure of 40 Mpa for 2 min to obtain a membrane pellet with a thickness of 5–15 mm. After pressing, the membrane pellet was sintered at 800 °C under an argon gas atmosphere with a flow rate of 300 ml/min.

2.2 Sample characterizations

In this work, powder X-ray diffraction analysis (XRD, Bruker D2 PHASER (USA)) with Cu Kα radiation (λ = 0.15406 nm) was used to determine the crystal structure of all samples. The particle size and morphology were characterized by transmission electron microscopy (TEM, EM902 Zeiss, West Germany), while the chemical composition was studied using dispersive Raman spectrometry (Bruker, UK). The CNFs@Ag nanocomposites showed high specific surface area, and pore volumes were investigated by the gas absorption technique (BET).

Table 1 Precursor ratios used for the preparation of membrane composite materials under each condition.

Sample	CNF (g)	$AgNO_3$ (g)	Ethanol (ml)
CNF	10	-	100
CNF@Ag10	10	1	100
CNF@Ag20	10	2	100
CNF@Ag40	10	4	100
CNF@Ag200	10	20	100

CNF= Carbon nanofibers, Ag= silver content added in nanofibers; 0%, 10%, 20%, 40% and 200%

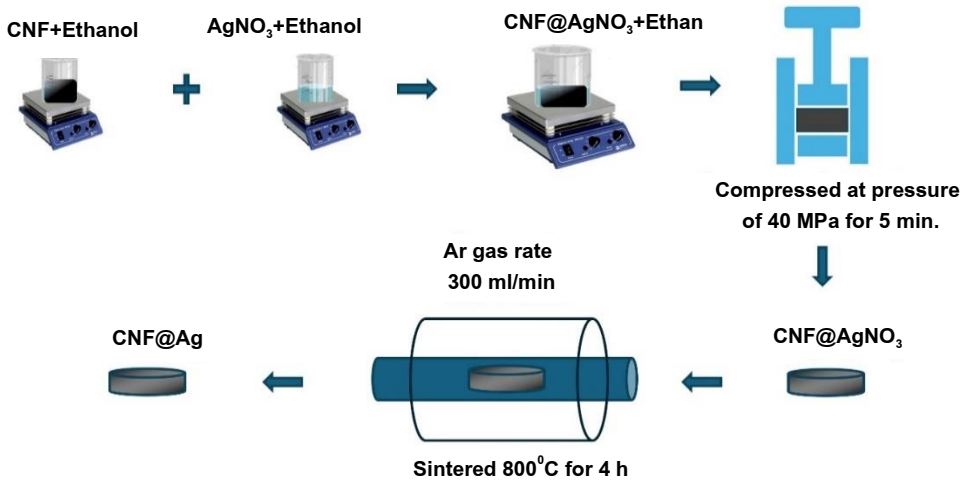

Figure 1 Precursor preparation process and membrane extrusion

2.3 Filtration rate test

The flow rate of water through the experimental membrane was tested using seawater and filtered using a Buchner filter set as shown in Figure 2, which was a dead-end filtration method. The solution was fed in perpendicular to each CNF@Ag membrane. The water was filtered using a vacuum pump at a constant pressure of -60 PSI, allowing water to flow through the membrane until it was soaked, and then the timer was started. Each membrane was timed for 30 min of filtration. The water obtained was measured with a measuring cylinder and the flow rate was calculated using the equation.

$$Q = \frac{V}{t} \quad (1)$$

Q is the flow rate of water through the membrane in m^3/min, V is the volume in m^3, and t is the time in min. While the flux of water through the membrane can be calculated from

$$\Phi = \frac{V}{AtP} \quad (2)$$

Φ is the water flow flux through the cross-section of the membrane in l/m^2h bar. A is the cross-sectional area of the membrane in m^2, t is the time in hours, and *P* is the pressure in bar.

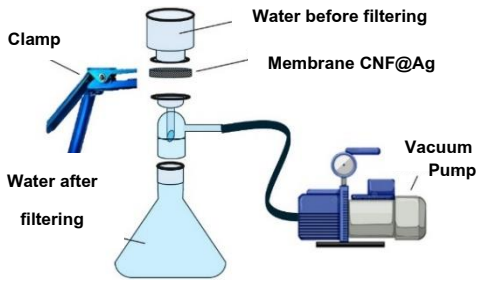

Figure 2 Water filter set with composite carbon nanofibers reinforced with

2.4 Study of the efficiency of turbidity removal in water

The efficiency of turbidity removal was studied after the water was filtered through each carbon nanofiber membrane reinforced with silver particles (CNF@Ag). The water filter setup was a modified Buchner vacuum filtration unit. Using the pressure reduction set up sped up the filtration, making it faster than normal filtration. The Buchner flask was connected to the membrane and funnel with a Buchner funnel clamp, with the filter funnel placed on top, and each CNF@Ag filter medium was placed between the funnel and the small arm, as can be seen in Figure 2. The small arm at the neck of the flask was connected to a vacuum pump to remove air from the flask.

2.5 Study of the efficiency of seawater salinity removal

The efficiency of removing salinity from seawater when filtered with the CNF@Ag composite carbon nanofiber membranes was studied. Seawater samples were collected in front of the lighthouse at Rajamangala University of Technology Srivijaya, Trang Campus, as shown in Figure 3.

Various parameters of seawater were measured before filtration, including temperature, pH, ORP, conductivity, turbidity, dissolved oxygen (DO), total dissolved solids (TDS), and salinity, using a Water Quality Monitor (Horiba). Then, after filtration, the seawater was tested again to measure the filtration efficiency of the experimental CNF@Ag membranes that had been incorporated into the Buchner filter setups.

3. Results and Discussion

3.1 Morphology of the membrane material of metal oxide carbon nanocomposite fibers

After being pressed by a hydraulic press at a pressure of 40 Mpa for 5 min and sintered at 800 °C under an argon gas atmosphere at a flow rate of 300 ml/min for 4 h, the membranes, with a diameter of approximately 26 mm and a thickness between 4-9 mm, were obtained as shown in Figure 4. The fabricated membranes had densities in the range of 2.36×10^{-6} -

2.96×10^{-6} kg/m^3, and the density values also increased with increasing amounts of silver particles.

Detailed analysis was conducted by mounting the membrane samples on a steel base before coating them with gold of a thickness of approximately 5 nm to increase their electrical conductivity. High- magnification images were taken using a scanning microscope. The scanning microscope images at magnifications of 1000x and 10,000x of the CNF@Ag fibers using 0%, 10%, 20%, 40% and 200% silver nitrate precursor are shown in Figure 5. The fibers of all samples had a random arrangement with no definite direction. The fiber sizes are analyzed using the ImageJ program; the average fiber size was 84.42±14.14 nm and the nanoparticles formed and distributed in the composite nanofiber can be observed adhering to the fiber surfaces, as clearly seen in Figure 6. The sizes of the fibers before and after calcination are summarized in Table 2.

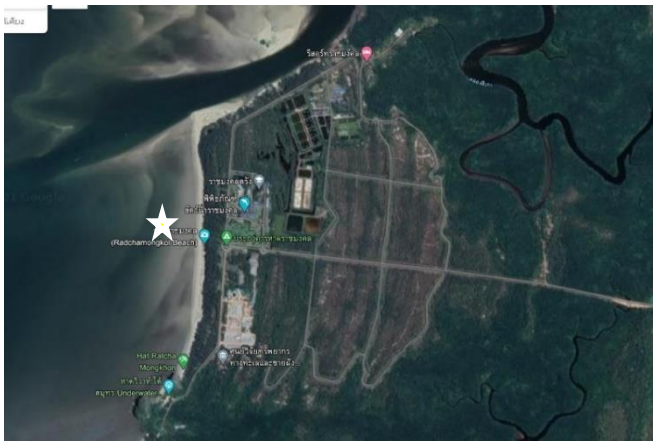

Figure 3 The points where seawater samples were collected from satellite imagery maps within Rajamangala University of Technology Srivijaya (Trang Campus)

Figure 4 Appearance and dimensions of a sintered membrane

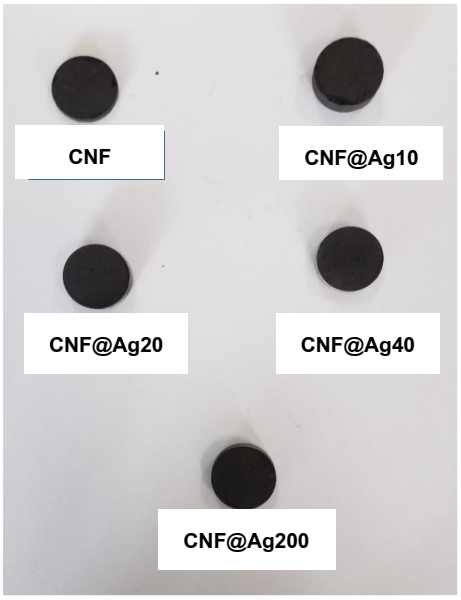

Figure 5 Membranes fabricated from CNF@Ag fibers with different silver particle addition rates. CNF= Carbon nanofiber, Ag= silver content added to the nanofibers; 0%, 10%, 20%, 40% and 200%

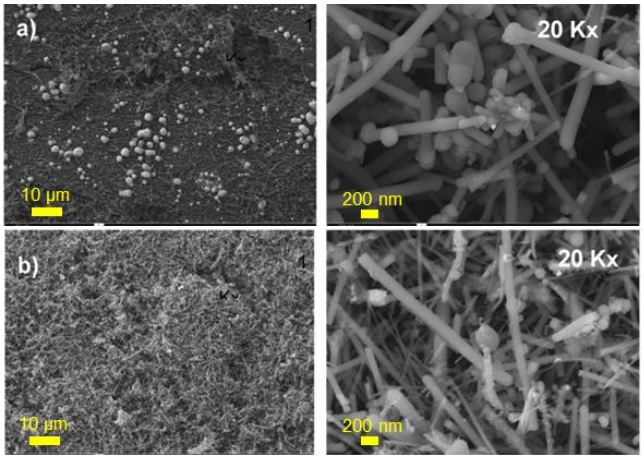

Figure 6 Scanning electron microscope images of the fabricated CNF@Ag metal oxide carbon nanocomposite membranes prepared using different concentrations of precursor: a) CNF@Ag200, b) CNF@Ag40, c) CNF@Ag20, d) CNF@Ag10, and e) CNF

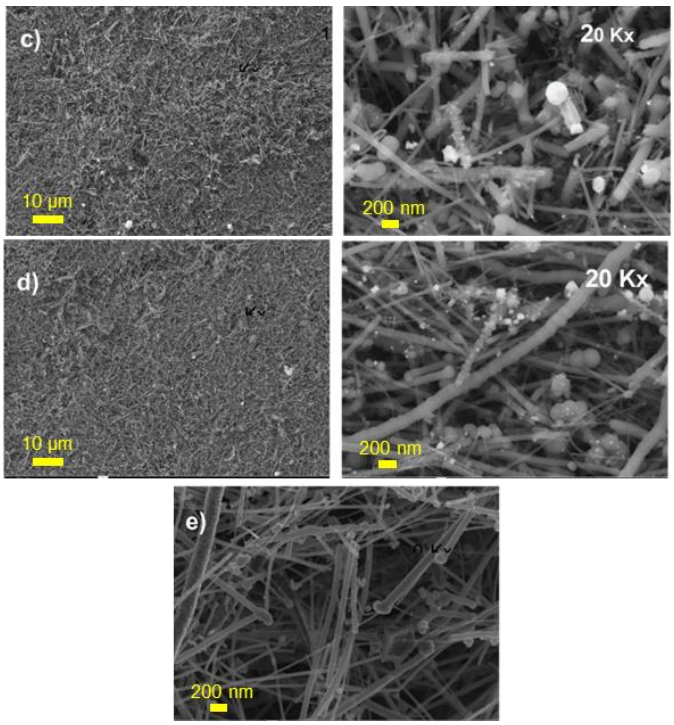

Figure 6 (Continuous)

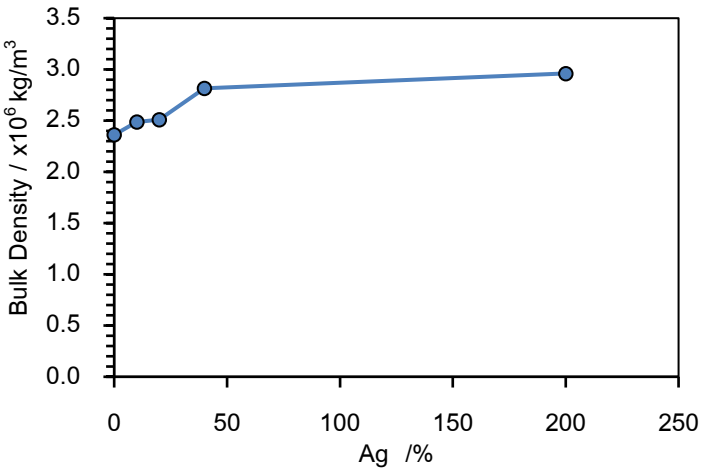

Figure 7 Density of membranes reinforced with different concentrations of silver particles

After degassing the samples at 300 C for 1 night, the specific surface area and porosity properties were measured using a Brunauer-Emmett-Teller analyzer at 77 K. The surface area and porosity were then evaluated by the BET method. It was found that the fibers reinforced with silver particles as shown in Figure 8 exhibited a hysteresis loop type IV adsorption and desorption pattern due to the condensation of nitrogen gas molecules in the mesoporous pores (Sinprachim *et al.*, 2016). The knee-shaped region at low pressure also indicated the presence of a large number of small pores, resulting in a higher specific surface area of the membrane compared to the CNF membrane without silver reinforcement. The low specific surface area of the membrane made from pure CNF may be due to the absence of silver particles, which made the pure CNF more homogeneous and dense when the membrane was compressed at a high pressure of 60 MPa. Meanwhile, compared to the membrane reinforced with particles, the membrane reinforced with fewer silver particles had a larger surface area because the silver nanoparticles were inserted between the fiber slits. Increasing the size and number of junctions between carbon nanofibers resulted in an increase in the pore volume, which had an effect on the increase in the specific surface area. However, the specific surface area decreased with an increase in the silver addition concentration. The membranes had specific surface areas ranging from 14.95 to 65.63 m2/g and pore sizes ranging from 9.21 to 21.99 nm, which might be due to the increase in the amount of silver particles, a very dense metal compared to the lightweight carbon fibers, causing the overall mass to increase significantly. Therefore, the calculated surface area to mass ratio was lower with the increase in the silver fraction, as summarized in Table 3.

Table 2 General properties of membranes.

Membranes	% of Ag composited	Mass (g)	Diameter (mm)	Thickness (mm)	Cross-sectional area ($x10^{-4}$ m^2)	Density ($x10^{-6}$ kg/m^3)
CNF	0	1.35	26±1.02	7.0±0.66	5.31	2.36
CNF@Ag10	10	1.32	26±1.24	6.5±0.88	5.31	2.42
CNF@Ag20	20	0.82	26±0.68	4±0.94	5.31	2.51
CNF@Ag40	40	0.92	26±0.72	4±0.28	5.31	2.82
CNF@Ag200	200	1.33	26±0.84	5.5±0.74	5.31	2.96

Table 3 Surface area and porosity of membranes fabricated with CNF@Ag composite at Ag concentrations of 0%, 10%, 20%, 40%, and 200%

Membranes	S_{BET} (m^2/g)	D_{mean} (nm)	V_{pore} (cm^3/g)
CNF	14.95	21.08	0.078
CNF@Ag10	65.63	9.21	0.151
CNF@Ag20	27.18	15.24	0.104
CNF@Ag40	20.21	18.46	0.093
CNF@Ag200	18.82	21.99	0.104

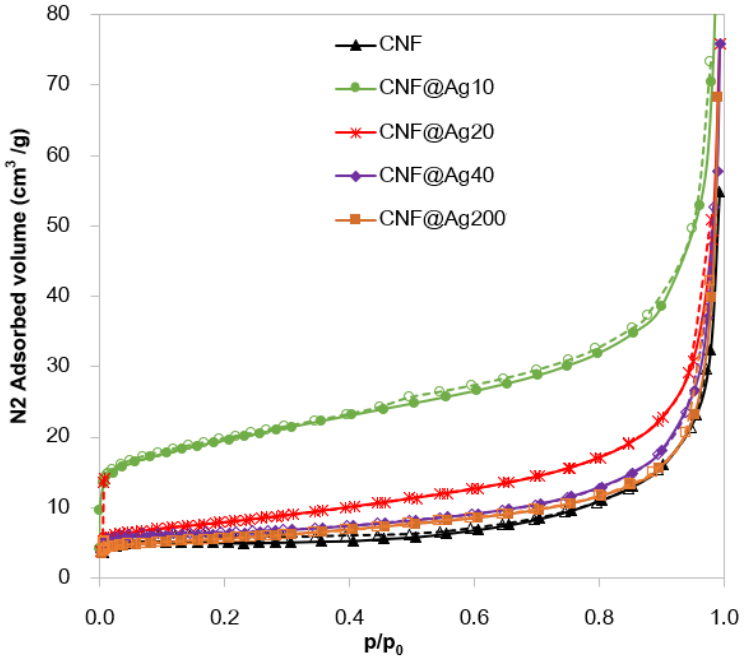

Figure 8 Graphs showing the adsorption and desorption of CNF fibers CNF@Ag10, CNF@Ag20, CNF@Ag40, and CNF@Ag200. CNF= Carbon nanofibers, Ag= silver content added to nanofibers: 0%, 10%, 20%, 40% and 200%

3.2 Structural analysis using X-ray diffraction technique

The study of structural property analysis was conducted using the X-ray diffraction technique with Cu-K radiation (λ = 0.15406 nm) in the range of 20-90°. From Figure 9, the X-ray diffraction pattern curves show the positions of carbon peaks at approximately 26° and 44°, representing the (002) and (101) diffraction planes, respectively, as per the carbon standard file PDF# 75-1621 (Shalaby *et al.*, 2015). In the case of CNF@Ag samples, the diffraction peaks of Ag were found at approximately 38.2°, 44.4°, 64.6°, 77.5°, and 81.7°, corresponding to the (111), (200), (220), (311), and (222) diffraction planes, respectively, of the silver standard file PDF# 87-0720 (Yuwen *et al.*, 2014), which were presumably consistent with the diffraction peaks of cubic Ag that was distributed in different positions according to the standard file as shown in Figure 9. It is noticeable that Ag did not form an oxide structure because it is an inert element. The effect of preparation with different concentrations of precursors did not affect the diffraction pattern but affected the intensity value, which was consistent with the samples of higher Ag concentration having higher spectral intensity (Dubey *et al.*, 2009).

3.3 Characterization of carbon using Raman spectroscopy

The Raman spectra were measured in the range of 100 – 4000 cm^{-1} using a 532 nm laser and are shown in Figure 10. The Raman spectra of the CNF and CNF metal oxide nanocomposites display common peaks related to carbon, namely, the G-Band peak at approximately 1590 cm^{-1} and the D-Band peak at approximately 1340 cm^{-1}. Moreover, for all samples, the peaks overlap and indicate the presence of amorphous carbon (Li *et al.*, 2016). The slightly visible peak in the range of 2600 – 2900 cm^{-1} is due to the phonon vibration of graphite crystals that are mixed in the sample (Kuzmany *et al.*, 2021).

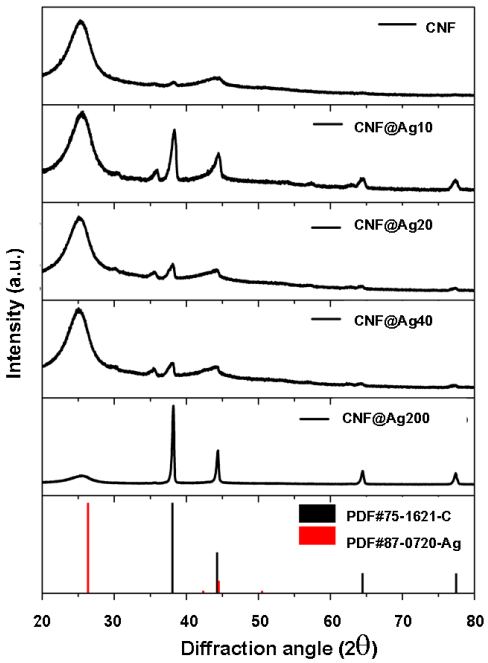

Figure 9 X-ray diffraction patterns of samples at different compositions and concentrations. CNF= Carbon nanofibers, Ag= silver content added to nanofibers; 0%, 10%, 20%, 40% and 200%

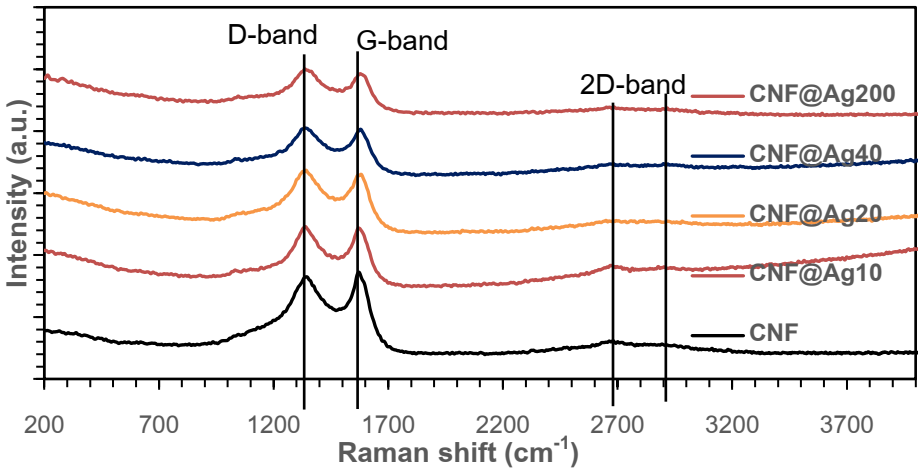

Figure 10 Raman spectra of the CNF carbon nanocomposite metal oxide fiber materials of CNF fibers CNF@Ag10%, CNF@Ag20%, CNF@Ag40%, and CNF@Ag200%. CNF= Carbon nanofibers, Ag= silver content added in nanofibers; 0%, 10%, 20%, 40% and 200%

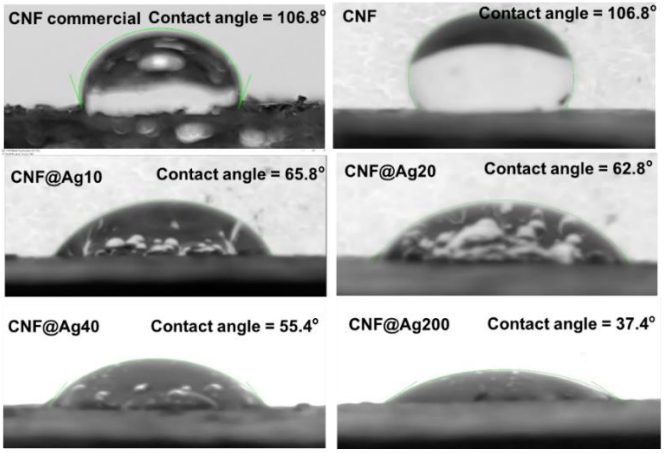

Figure 11 Images of water droplets on the surface of the prepared membrane. CNF= Carbon nanofibers, Ag= silver content added to nanofibers: 0%, 10%, 20%, 40% and 200%

3.4 Water absorption capacity of the membranes and wettability of the surface

The contact angle measurement experiment was used to study the wetting properties of the membranes. As shown in Figure 11, the CNF-based membranes had the highest contact angle value of only 106.8°, which highlighted the hydrophobic surface properties of the pure CNF (Zhang *et al.*, 2020). Meanwhile, in the case of the CNF-Ag composites, the contact angle values decreased with the increasing proportion of silver particles as shown in Figure 12. In other words, with the addition of silver particles, the membranes were better wet. However, after immersion in water for 15 h, the water absorption properties of the membranes were found to be close, in the range of 279.34–288.27%, as shown in Table 4, which may have been because the membranes had similar specific surface areas, and the immersion time of up to 15 h was long enough for the membranes to fully absorb water.

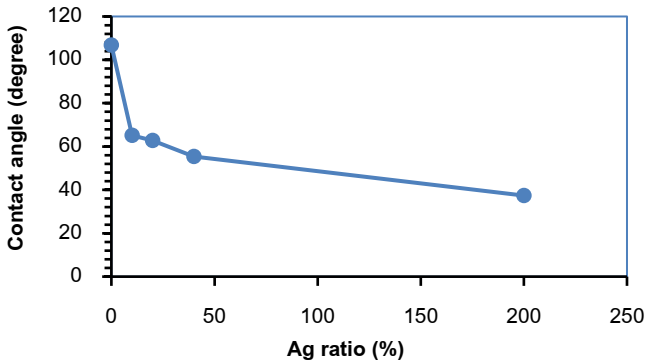

Figure 12 Graph showing the relationship between contact angle and Ag addition amount

Table 4 Water absorption and contact angle measurements of the prepared membranes.

Membranes	Water absorption rate compared to the mass of the membrane (%)
CNF	281.61
CNF@Ag10	286.59
CNF@Ag20	288.27
CNF@Ag40	279.34
CNF@Ag200	287.26

CNF= Carbon nanofibers, Ag= silver content added to the nanofibers; 0%, 10%, 20%, 40% and 200%

Table 5 Results of the study on water flow rate through CNF and CNF@Ag membranes.

Membranes	Flow rate (ml/min)	Flux (l/m^{2}hbar)
CNF	5.56	50.04
CNF@Ag10	4.17	113.74
CNF@Ag20	5.08	138.43
CNF@Ag40	5.39	146.23
CNF@Ag200	5.56	151.65

Table 6 Seawater parameters before CNF and CNF@Ag membrane filtration.

Order	Parameter	Value	Unit
1	Temperature	32.57	°C
2	Acidity-Alkalinity	7.66	
3	ORP	198	mV
4	Conductivity	47.4	µs/cm
5	Turbidity	16.5	NTU
6	Dissolved Oxygen (DO)	8.84	mg/L
7	Total Dissolved Solids (TDS)	28.9	g/L
8	Salinity	30.8	ppt

CNF= Carbon nanofibers, Ag= Silver content added to nanofibers; 0%, 10%, 20%, 40% and 200%

3.5 Testing of water flow rate through the membrane

The results of the study of the flow rate of water through the composite nanocarbon fiber membranes were obtained by making the water flow through the vacuum filter set. The water was poured into the vacuum filter funnel, and the pressure was set to -60 PSI. The water slowly flowed through the membrane. The time was set with a stopwatch for 30 min. The volume of water that flowed into the flask was measured with a measuring cylinder. The volume of water obtained was recorded, calculated, and the results were compared as shown in Table 5. It is noticeable that pure carbon gave good flow rate values as well as the silver particle mixture up to 200%, while the mixture of small proportions of nanoparticles gave lower flow rate values respectively. However, this interesting result will be further studied in the future.

3.6 Study of removal rate of specific contaminants

The removal of salt and turbidity from seawater was investigated using a membrane filtration technique to evaluate membrane efficiency under different conditions. In the experiment, the seawater had parameters as listed in Table 6. The turbidity removal efficiency was evaluated by filtering water with an initial turbidity of 33.00 NTU through the experimental membrane using vacuum filtration at a pressure of -60 PSI (Muthuraman and Sasikala, 2014). The results indicated that turbidity could be effectively removed by the CNF@Ag membrane, with removal efficiencies ranging from 71.19% to 92.69% in all cases. Filtration through the experimental membrane yielded water with clarity of less than 10 NTU, which meets the drinking water quality criteria for turbidity set by the Ministry of Public Health (2000, 2011 edition). These results are summarized in Table 7.

The turbidity filtration process was classified as microfiltration, indicating that colloidal particles, emulsions, and suspended

solids were removed through pores with a size range of 0.05 to 20 μm. In addition, the addition of silver particles at higher ratios was found to significantly improve filtration efficiency. This improvement may be attributed to the reduction in interfiber gaps resulting from the insertion of silver nanoparticles, which enhances the capture of colloidal particles, as suggested by Praveen Kamath *et al.* (2023).

However, the experimental results shown in Table 8 indicate that all the membranes are ineffective in reducing salinity. These inefficiencies may be due to the filtration mechanism, which is influenced by the large interfiber gaps of 0.05 to 20 μm, as observed in the high-magnification scanning electron microscope (SEM) images (Figure 6). These gaps are larger than the size of the salt molecules, which is approximately 0.283 nm. In addition, the good wetting properties of the membrane allow water to easily permeate the membrane, enabling the salt molecules to pass through the membrane without being trapped. Therefore, the salinity values before and after filtration are similar, indicating that the salinity is not significantly reduced.

Table 7 Study of water turbidity reduction performance of different types of CNF@Ag membranes.

Membranes	Turbidity before filtration (NTU)	Turbidity after filtration (NTU)	Turbidity removal efficiency (%)
CNF	33.00±0.12	7.53±0.60	76.47
CNF@Ag10	33.00±0.12	9.22±1.88	71.19
CNF@Ag20	33.00±0.12	3.65±0.62	88.59
CNF@Ag40	33.00±0.12	2.56±0.48	92.00
CNF@Ag200	33.00±0.12	2.34±0.26	92.69

CNF= Carbon nanofibers, Ag= silver content added to nanofibers; 0%, 10%, 20%, 40% and 200%

Table 8 Comparison of salinity values before and after filtration with different types of membranes.

Membranes	Salinity before filtration (%)	Salinity after filtration (%)
CNF	30±0.8	30±0.6
CNF@Ag10	30±0.8	30±0.8
CNF@Ag20	30±0.8	30±0.4
CNF@Ag40	30±0.8	30±0.8
CNF@Ag200	30±0.8	30±0.6

4. Conclusion

In this study, a binder-free extrusion process successfully fabricated a membrane, which was sintered at 800 °C, resulting in a cross-sectional area of 2.51 × 10^{-4} m². The membrane exhibited a smooth surface and a uniform distribution of silver nanoparticles on the carbon nanofiber (CNF) structure. The incorporation of silver nanoparticles significantly increased the membrane's density and reduced its specific surface area from 65.63 m²/g to 18.82 m²/g, while also enhancing its hydrophilicity. Filtration tests at -60 PSI revealed water flow rates ranging from 1.83 to 5.56 mL/min, with the membrane achieving a turbidity removal efficiency of 92.69%, thereby meeting drinking water quality standards. However, the membrane was found to be ineffective for desalination due to its pore size range of 9.21 to 21.99 micrometers, which is suitable for microfiltration but inadequate for separating smaller particles, such as salt molecules (0.283 nm). In conclusion, while the CNF@Ag membrane demonstrates promising results for microfiltration applications, further optimization is needed to enhance its desalination performance. Specifically, reducing the pore size and increasing the membrane thickness could improve its ability to filter smaller solutes, such as salts, thereby enabling more efficient desalination.

5. Acknowledgments

This research project was successfully implemented with the support of the research budget by Fundamental Fund (FF) via Rajamangala University of Technology Srivijaya in 2020 (Project code 312). We also acknowledge the editorial team at the Office of Academic Journal Administration, KMITL, for proofreading this manuscript.

6. References

Andrade, P.F., de Faria, A.F., Oliveira, S.R., Arruda, M.A.Z. and do Carmo Gonçalves, M. 2015. Improved antibacterial activity of nanofiltration polysulfone membranes modified with silver nanoparticles. **Water Research** 81: 333-342.

Boretti, A. and Rosa, L. 2019. Reassessing the projections of the world water development report. **NPJ Clean Water** 2(1): 15.

Brown, C.M., Lund, J.R., Cai, X., Reed, P.M., Zagona, E.A., Ostfeld, A., Hall, J., Characklis, G.W., Yu, W. and Brekke, L. 2015. The future of water resources systems analysis: toward a scientific framework for sustainable water management. **Water Resources Research** 51(8): 6110-6124.

Davari, S., Omidkhah, M. and Salari, S. 2021. Role of polydopamine in the enhancement of binding stability of TiO2 nanoparticles on polyethersulfone ultrafiltration membrane. **Colloids and Surfaces A: Physicochemical and Engineering Aspects** 622: 126694.

Dubey, M., Bhadauria, S. and Kushwah, B. 2009. Green synthesis of nanosilver particles from extract of Eucalyptus hybrida (safeda) leaf. **Digest Journal of Nanomaterials and Biostructures** 4(3): 537-543.

Flörke, M., Schneider, C. and McDonald, R.I. 2018. Water competition between cities and agriculture driven by climate change and urban growth. **Nature Sustainability** 1(1): 51-58.

Gong, W., Bai, L. and Liang, H. 2024. Membrane-based technologies for removing emerging contaminants in urban

water systems: Limitations, successes, and future improvements. **Desalination** 590: 117974.

Gude, V.G. 2016. Desalination and sustainability an appraisal and current perspective. **Water Research** 89: 87-106.

Hulicova-Jurcakova, D., Li, X., Zhu, Z., De Marco, R. and Lu, G.Q. 2008. Graphitic carbon nanofibers synthesized by the chemical vapor deposition (CVD) method and their electrochemical performances in supercapacitors. **Energy & Fuels** 22(6): 4139-4145.

Idumah, C.I. and Hassan, A. 2016. Emerging trends in graphene carbon based polymer nanocomposites and applications. **Reviews in Chemical Engineering** 32(2): 223-264.

Inagaki, M., Yang, Y. and Kang, F. 2012. Carbon nanofibers prepared via electrospinning. **Advanced materials** 24(19): 2547-2566.

Kuzmany, H., Shi, L., Martinati, M., Cambré, S., Wenseleers, W., Kürti, J., Koltai, J., Kukucska, G., Cao, K. and Kaiser, U. 2021. Well-defined sub-nanometer graphene ribbons synthesized inside carbon nanotubes. **Carbon** 171: 221-229.

Levchenko, I., Baranov, O., Riccardi, C., Roman, H.E., Cvelbar, U., Ivanova, E.P., Mohandas, M., ŠČajev, P., Malinauskas, T. and Xu, S. 2023. Nanoengineered Carbon‐Based Interfaces for Advanced Energy and Photonics Applications: A Recent Progress and Innovations. **Advanced Materials Interfaces** 10(1): 2201739.

Li, Y., Hu, Y.S., Li, H., Chen, L. and Huang, X. 2016. A superior low-cost amorphous carbon anode made from pitch and lignin for sodium-ion batteries. **Journal of Materials Chemistry A** 4(1): 96-104.

Muthuraman, G. and Sasikala, S. 2014. Removal of turbidity from drinking water using natural coagulants. **Journal of Industrial and Engineering Chemistry** 20(4): 1727-1731.

Noamani, S., Niroomand, S., Rastgar, M. and Sadrzadeh, M. 2019. Carbon-based polymer nanocomposite membranes for oily wastewater treatment. **NPJ Clean Water** 2(1): 20.

Oladunni, J., Zain, J.H., Hai, A., Banat, F., Bharath, G. and Alhseinat, E. 2018. A comprehensive review on recently developed carbon based nanocomposites for capacitive deionization: from theory to practice. **Separation and Purification Technology** 207: 291-320.

Pavlenko, V., Żółtowska, S., Haruna, A., Zahid, M., Mansurov, Z., Supiyeva, Z., Galal, A., Ozoemena, K., Abbas, Q. and Jesionowski, T. 2022. A comprehensive review of template-assisted porous carbons: Modern preparation methods and advanced applications. **Materials Science and Engineering: R: Reports** 149: 100682.

Praveen Kamath, P., Sil, S., Truong, V.G. and Nic Chormaic, S. 2023. Particle trapping with optical nanofibers: a review. **Biomedical Optics Express** 14(12): 6172-6189.

Rahimpour, A., Madaeni, S., Taheri, A. and Mansourpanah, Y. 2008. Coupling TiO2 nanoparticles with UV irradiation for modification of polyethersulfone ultrafiltration membranes. **Journal of Membrane Science** 313(1-2): 158-169.

Razmjou, A., Mansouri, J. and Chen, V. 2011. The effects of mechanical and chemical modification of TiO2 nanoparticles on the surface chemistry, structure and fouling performance of PES ultrafiltration membranes. **Journal of Membrane Science** 378(1-2): 73-84.

Shalaby, A., Nihtianova, D., Markov, P., Staneva, A., Iordanova, R. and Dimitriev, Y. 2015. Structural analysis of reduced graphene oxide by transmission electron microscopy. **Bulgarian Chemical Communications** 47(1): 291-295.

Sinprachim, T., Phumying, S. and Maensiri, S. 2016. Electrochemical energy storage performance of electrospun AgO_x-MnO_x/CNF composites. **Journal of Alloys and Compounds** 677: 1-11.

Williams, J. 2022. Desalination in the 21st century: a critical review of trends and debates. **Water Alternatives** 15(2): 193-217.

Yang, Q. and Mi, B. 2013. Nanomaterials for membrane fouling control: accomplishments and challenges. **Advances in Chronic Kidney Disease** 20(6): 536-555.

Yu, Y., Zhou, Z., Huang, G., Cheng, H., Han, L., Zhao, S., Chen, Y. and Meng, F. 2022. Purifying water with silver nanoparticles (AgNPs)-incorporated membranes: Recent advancements and critical challenges. **Water Research** 222: 118901.

Yuwen, L., Xu, F., Xue, B., Luo, Z., Zhang, Q., Bao, B., Su, S., Weng, L., Huang, W. and Wang, L. 2014. General synthesis of noble metal (Au, Ag, Pd, Pt) nanocrystal modified MoS 2 nanosheets and the enhanced catalytic activity of Pd–MoS 2 for methanol oxidation. **Nanoscale** 6(11): 5762-5769.

Zhang, S., Huang, X., Wang, D., Xiao, W., Huo, L., Zhao, M., Wang, L. and Gao, J. 2020. Flexible and superhydrophobic composites with dual polymer nanofiber and carbon nanofiber network for high-performance chemical vapor sensing and oil/water separation. **ACS Applied Materials & Interfaces** 12(41): 47076-47089.